

Solar Panel Motor Tracker Model Comparison Between PID and Fuzzy PD

Fitri Rahmah*[‡], Fitriahidayanti*, Erna Kusuma Wati*, Kiki Rezki
Lestari*, Sapto Wahyu Sudrajat**

*Engineering Physics Study Program, Faculty of Engineering and Science, Universitas Nasional,
Jakarta – Indonesia 12520

**Electrical Engineering Study Program, Faculty of Intelligent Electrical and Informatics
Technology, Institut Teknologi Sepuluh Nopember, Surabaya – Indonesia 60111

(fitri.rahmah@civitas.unas.ac.id, fitriahidayanti@gmail.com, ernakusuma.w@gmail.com,
kikirezkilestari@gmail.com, saptowahyusudrajat@gmail.com)

[‡] Corresponding Author; Fitri Rahmah, Engineering Physics Study Program, Faculty of
Engineering and Science, Universitas Nasional, Jakarta – Indonesia 12520, +62-82245993848,
fitri.rahmah@civitas.unas.ac.id

Received: 25.05.2022 Accepted: 21.08.2022

Abstract- Solar panels are one alternative to overcome energy scarcity. Solar panel optimization is necessary to maximize the amount of solar energy absorbed. Solar panel tracker motors are one method of ensuring that the position of sunlight collectors is always aligned with the sun's direction. This article discusses Proportional-Integral-Derivative (PID) and fuzzy Proportional-Derivative (PD) controller models for tracking solar panels. There are two conditions tested, namely with and without noise. For both tests, the fuzzy PD controller model had a faster settling time of 8,480 s in the absence of noise and 6,388 s in the presence of noise. Furthermore, the optimal performance of the PI and PID controllers, which show an overshoot on the motor angle position response, has been corrected by the Fuzzy controller with PD gain.

Keywords Solar panel tracker; Proportional-Integral-Derivative (PID) control; Fuzzy Logic Control (FLC); Fuzzy PD.

1. Introduction

Solar panels generate energy based on the position and direction of the sun. Solar panel use is still generally inefficient, encouraging additional research and development efforts. One of the concepts associated with using a tracking solar panel is adjusting the position of the solar collector so that it is continuously facing the sun [1-6]. Tracking the sun's position can be accomplished passively, through the thermal expansion of solar panels, or actively by using DC motors, gearboxes, and other components.

The dual-axis automatic tracking system helps optimize solar energy from four directions and improve conversion efficiency [7]. The working principle of two-axis automatic tracking is identical to the working principle of a single-axis tracking system. A significant distinction between the two is that solar panels in dual-axis systems follow the direction of sunlight from east to west and the high position of sunlight's angle in the sky, but single-axis systems do not [8]. The

electrical energy generated by traced solar panels can power various methods, including hydroponic systems [9-11].

Hydroponic farming can produce various crops, but it requires energy and time to regulate irrigation, lighting, room temperature, nutrient water levels, electroconductivity, and pH [12-13]. According to [14], hydroponics consumes 11 times the electrical energy required for conventional farming. As a result, it is necessary to power a hydroponic system with traced solar panels.

A combination of Proportional-Derivative (PD) controllers and Fuzzy Logic Control (FLC) is used to determine the requirement for effective controllers. The advantage of the PD controller is its ease of implementation. By contrast, the FLC concept effectively deals with complex nonlinear systems with difficult-to-model uncertainties [15]. Although the FLC controller is straightforward to design, it has several drawbacks, including the method's limitations in analysis and synthesis. The PID control system is modified to enhance the system's performance [16-17]. The

performance of the system can be observed in various time domain specifications [18].

This article will describe how to implement a position control system on solar panels using Fuzzy PD and PID modeling to obtain a reliable alternative control system. This paper aims to demonstrate Fuzzy PD and PID modeling to create a reliable alternative control system for solar panels. The fuzzy PD was selected since the DC motor oscillates a lot, possibly requiring the application of a derivative method to compensate for fluctuations. Model in Simulink with a fuzzy PD structure. The first step is to run a non-interference test on each PID and Fuzzy PD controller. In comparison, the Fuzzy PD controller takes slightly longer to reach the set point but responds faster due to the lack of overshoot.

2. Materials and Methods

2.1. Solar Tracker

Automatic solar trackers with single-axis tracking move the solar panel from east to west concerning the changes in a sun's motion across the horizontal axis [19,20]. Furthermore, dual-axis tracking involves movement on both the vertical and horizontal axis. Compared to automatic search on single-axis solar panels, this technology maximizes energy generation by maintaining solar panels perpendicular to direct sunlight.

The position control system model in the solar panel system is illustrated in Fig.1 [21]. The system's operating principle is to adjust the PV panel position to track the sun continuously. As a result, the solar-collecting plate's surface is always perpendicular to the direction of the sun's rays because sunlight falling on a vertical panel surface will produce the maximum amount of energy, 1000 W/m² or 1 kW/m² [22].

The system input is the rate of sunlight (θ_i) received by the LDR sensor, which is placed in such a way on the solar panel [21]. Meanwhile, the system's output is the angular position of the motor (θ_o), which is used to rotate the solar panel in the direction of the sun.

Because the solar panel's objective is the sun, it must be able to track the sun's motion to maximize the solar panel's efficiency. A controllable solar panel is required to ensure that the solar panels are always perpendicular to the sun. Modeling is accomplished by deriving mathematical equations from the solar panels' constituent parts.

2.2. DC Motor Modelling

In a solar tracker system, the solar panels are positioned by a DC motor whose position is adjusted in response to the input voltage. In general, the DC motor model is shown in Fig.2. The DC motor's input is in the form of voltage (V),

while the output is in the form of the motor shaft's angular position (θ). The following parameters apply to DC motors.

1. J_{mot} : Moment of Inertia (kg.m²);
2. b_{mot} : Coefficient of viscosity (Nm.sec);
3. K_{emf} : Coefficient of back EMF (V/rad/sec);
4. K_{τ} : Torque (Nm/A);
5. R : Resistance (Ω);
6. L_{ind} : Inductance (H).

The motor's torque is directly proportional to the amount of current it receives, as shown in Eq. (1),

$$Torque = K_{\tau}I. \tag{1}$$

The shaft's angular velocity is directly proportional to the back emf (e), which has K_{emf} , thus,

$$e = K_{emf}\dot{\phi}. \tag{2}$$

In the SI units, motor torque and back emf have the same value, namely $K = K_{\tau} = K_{emf}$. The Simulink model can be created by considering Kirchhoff's law,

$$\iint \frac{d^2\phi}{dt^2} dt = \int \frac{d\phi}{dt} dt = \phi \tag{3}$$

$$\int \frac{dI}{dt} dt = I \tag{4}$$

$$J_{mot} \frac{d^2\phi}{dt^2} = -b_{mot} \frac{d\phi}{dt} + T_{mot} \Rightarrow \frac{d^2\phi}{dt^2} = \frac{1}{J_{mot}} \left(-b_{mot} \frac{d\phi}{dt} + K_{\tau}I \right) \tag{5}$$

$$L_{ind} \frac{dI}{dt} = V - RI - e \Rightarrow \frac{dI}{dt} = \frac{1}{L_{ind}} \left(V - RI - K_{emf} \frac{d\phi}{dt} \right) \tag{6}$$

By setting the parameter values in Table 1, the Simulink model of the motor can be described according to Fig.3.

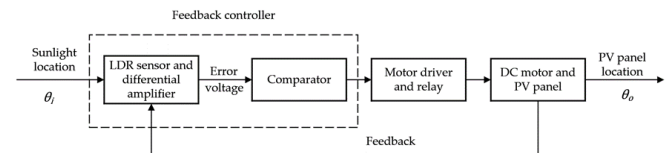


Fig. 1. Schematic of the solar panel system.

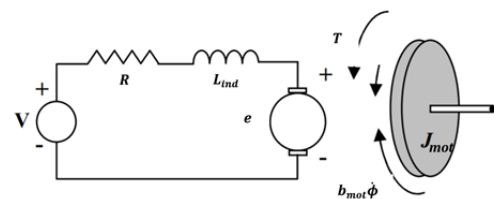


Fig. 2. Schematic of DC motor.

Table 1. Solar panels and DC motors parameters.

Solar Panel Parameters	DC Motor Parameters
Mass, $m = 50 \text{ kg}$	Back EMF Constant, $K_{emf} = 0.44 \text{ V}/(\text{rad}/\text{s})$
Width, $w = 1.04 \text{ m}$	Torque Constant, $K_T = 37.69 \text{ Nm}/\text{A}$
Length, $l = 1.4 \text{ m}$	Inductance, $L_{ind} = 0.11 \text{ H}$
Depth, $d = 0.1 \text{ m}$	Resistance, $R = 17.45 \Omega$
Areas, $A = 1.46 \text{ m}^2$	Gear Ratios, $K_g = 300$
Elevation angle, $\beta = 0.79 \text{ rad}$	-
Constant damping, $K_d = 5 \text{ Nm}/(\text{rad}/\text{s})$	-
Inertia, $J = 8.68 \text{ kgm}^2$	-

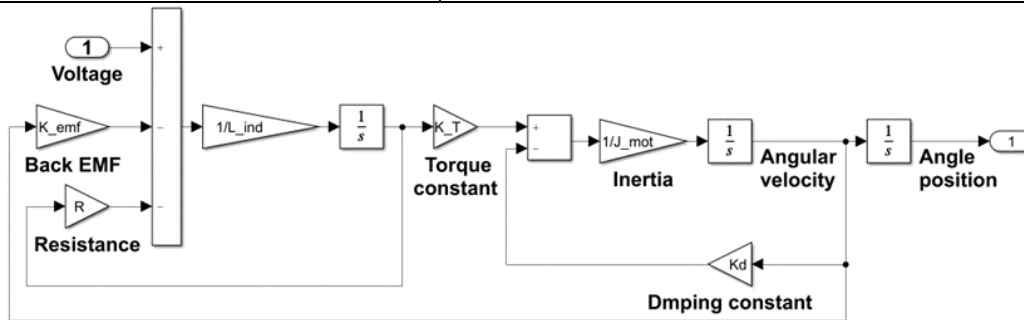


Fig. 3. Simulink model DC motor position control.

2.3. Fuzzy Modelling

To improve the performance of the PID control system, we can make modifications using PD-based FLC, and the system was renamed Fuzzy PD according to the rules specified in Table 2. The terms BIG_N (big negative), MED_N (medium negative), SMALL_N (slight negative), ZERO, SMALL_P (small positive), MED_P (medium positive), and BIG_P (big positive) are used to group membership functions. The membership function's input range for error (e) and delta error (Δe) is -50 to 50, while the control output range is -100 to 100. Once the variables for each membership function are known, the membership function is designed using the Gaussian method for the error (e) variable, delta error (Δe), and control output, as illustrated in Fig.4 – Fig.6.

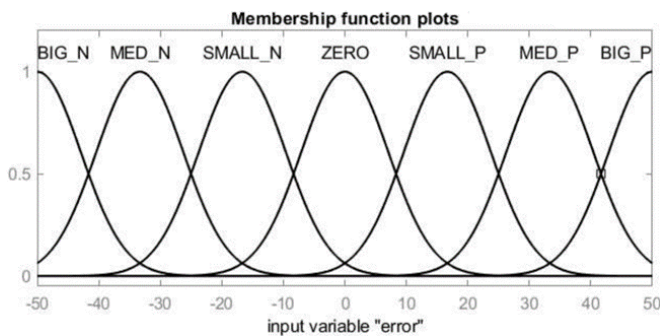


Fig. 4. Error (e) membership function.

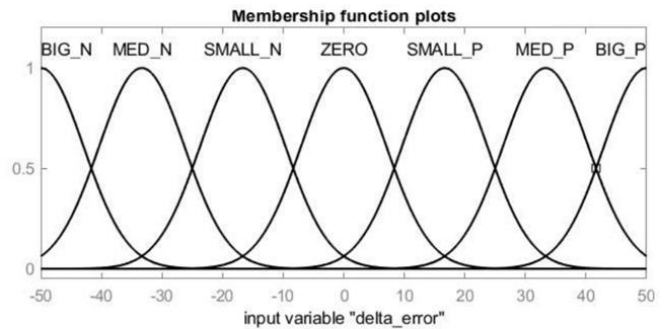


Fig. 5. Delta error (Δe) membership function.

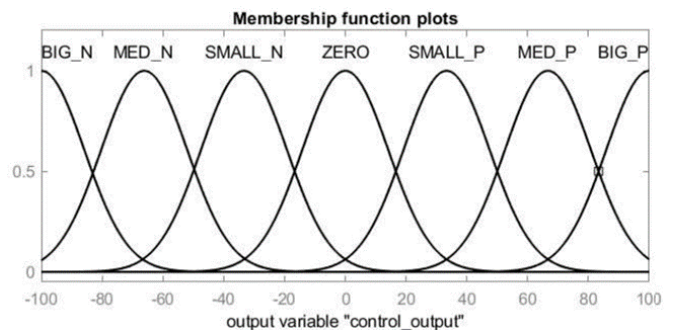


Fig. 6. Output control membership function.

Following the development of the membership function and fuzzy rules, the next step is to implement the MATLAB block diagrams and fuzzy designs. Figure 7 illustrates the results of the Fuzzy PD and PID controller design on Simulink, where the system circuit is a closed-loop system.

Table 2. Fuzzy PD rule base.

$\Delta e \backslash e$	BIG_N	MED_N	SMALL_N	ZERO	SMALL_P	MED_P	BIG_P
BIG_N	BIG_N	BIG_N	BIG_N	MED_N	SMALL_N	SMALL_N	ZERO
MED_N	BIG_N	MED_N	MED_N	MED_N	SMALL_N	ZERO	SMALL_P
SMALL_N	BIG_N	MED_N	SMALL_N	SMALL_N	ZERO	SMALL_P	MED_P
ZERO	BIG_N	MED_N	SMALL_N	ZERO	SMALL_P	MED_P	BIG_P
SMALL_P	MED_N	SMALL_N	ZERO	SMALL_P	SMALL_P	MED_P	BIG_P
MED_P	SMALL_N	ZERO	SMALL_P	MED_P	MED_P	MED_P	BIG_P
BIG_P	ZERO	SMALL_P	SMALL_P	MED_P	BIG_P	BIG_P	BIG_P

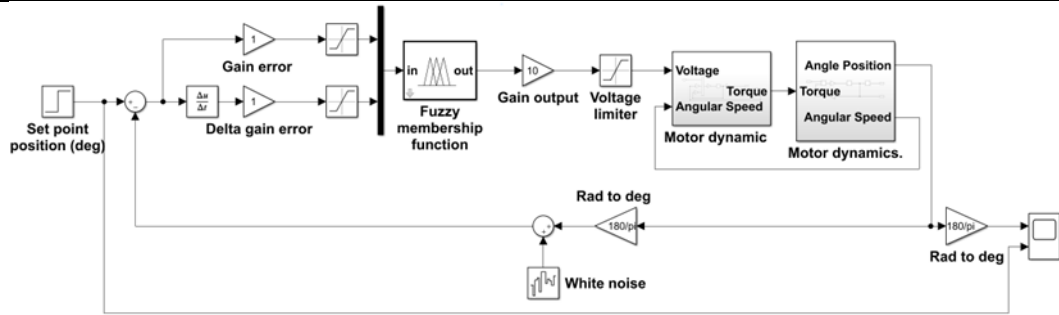


Fig. 7. Fuzzy PD structure Simulink model.

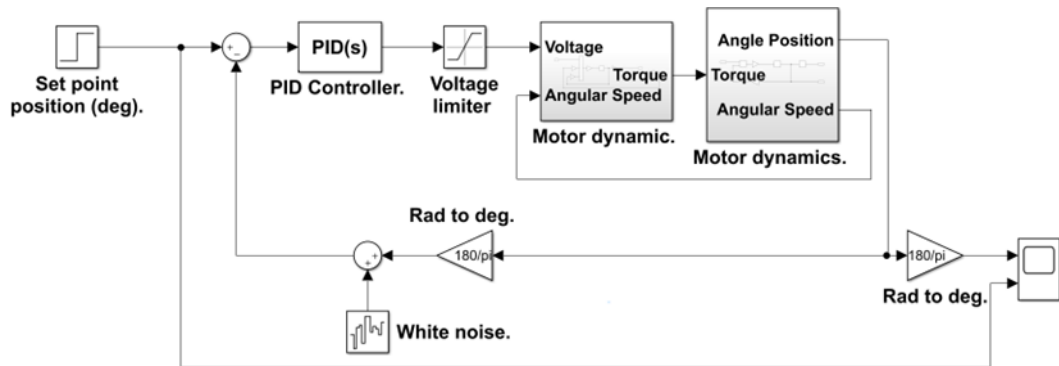


Fig. 8. PID structure Simulink model.

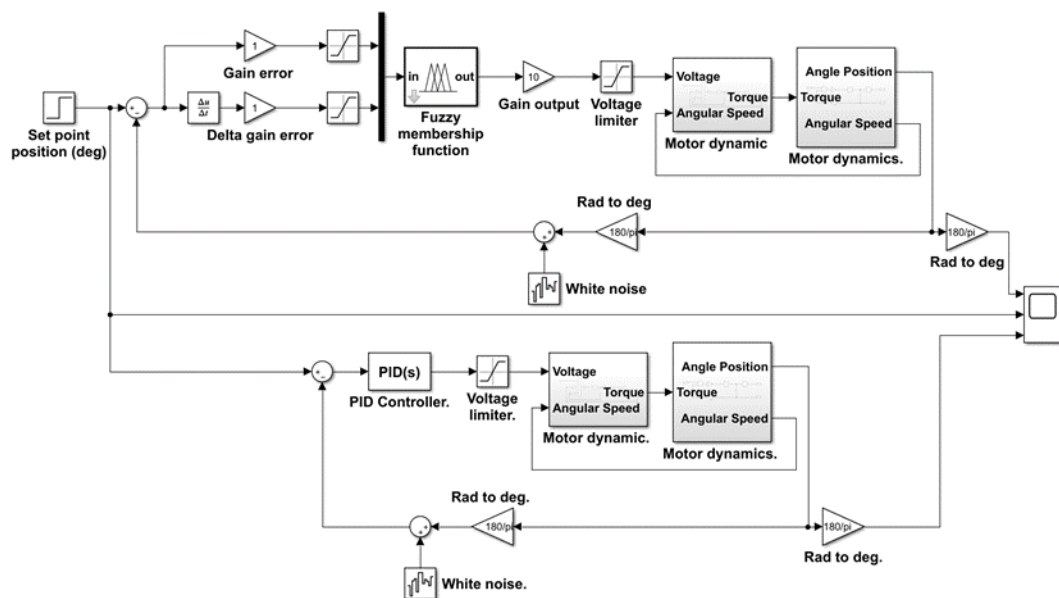


Fig. 9. Combined Simulink PID and Fuzzy PD structure models with 0.1-degree noise variance.

2.4. PID and Fuzzy PD Modelling

Fuzzy PD was chosen because the DC motor exhibits a high degree of oscillation, necessitating a derivative method to correct the fluctuations. In this model, the membership function has two inputs: error (e) and delta error (Δe). At the same time, the output is in the form of voltage. This model contains three gains: KE, KD, and ALPHA. If Simulink is used to visualize it, it will appear in Fig.7. Meanwhile, in the PID model, P is set to 0.0798, I is set to 0.0144, and D is set to 0.0882. Figure 8 illustrates the Simulink visualization.

2.5. Combined PID and Fuzzy PD Modelling with Additional 0.1-degree Measurement Noise

PID and Fuzzy PD models are combined in this modeling. The analysis was conducted with an additional noise variance of 0.1 degree from the system's feedback readings range. Figure 9 illustrates this model.

3. Results

In this simulation, the motor angle on the solar panel is monitored in real-time. Prior to the performance test on the PID controller and Fuzzy PD controller, an open loop test is performed on the motor with voltage input and motor angle output. All response results and dynamic models are simulated using MATLAB software with the following comparative simulation results.

3.1. Open Loop Test

In an open-loop test, the system is conducted by applying a 1 V input voltage. The test response is depicted in Fig.10. The open-loop test results indicate that the speed response reaches 20.8 deg/s with a 1 V input. This test aims to analyze the plant's characteristics to facilitate linguistic analysis during the fuzzy controller design process. Under the speed response, the position response also increases. For instance, at a speed of 20.8 deg/s, it will achieve a position of approximately 180 degrees in ten seconds. Figure 11 illustrates the position response.

3.2. Comparative Test Results on PID and Fuzzy PD Controllers

Figures 7 and Figure 8 show the block diagrams of the fuzzy PD and PID controllers, where the performance of the two controllers will be compared in this simulation. Two conditions are evaluated: testing without interference and testing with interference. These are used to determine the control system's robustness in the face of uncertainty by observing and analyzing system performance. The first is a non-interference test on each PID and Fuzzy PD controller. PID controller with parameters K_p 0.0798, K_i 0.0144, and K_d 0.0882 was previously obtained from the autotuning feature in the Simulink PID block. Given a set point of 30 degree, the dynamic response of the motor with this controller is shown in Fig.12.

Furthermore, in the fuzzy PD controller, the error and delta error data are used as input for the fuzzy membership function, as shown in Fig.4 and Fig.5. The membership function represents the input error and delta error. The processing results of this membership function will become a linguistic structure and will be needed to evaluate the rule base in Table 2. Rule evacuation will produce output according to the membership output, which has a range of -100 to 100, where this value states the size of the PWM signal given to the motor as shown in Fig.6. This fuzzy system's final process is called defuzzification, where the linguistic variables from the rule evacuation will be used as the actual output value. The results of the dynamic response of the PD fuzzy controller with a motor angle position set point of 30 degrees are shown in Fig.13. The results of the comparison of the dynamic response of the two controllers are shown in Fig.14.

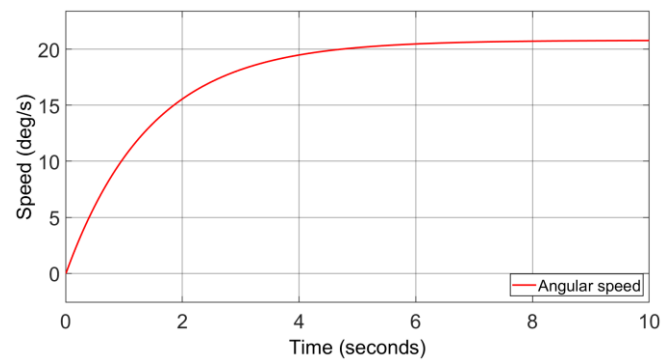


Fig. 10. Open loop test angular velocity response.

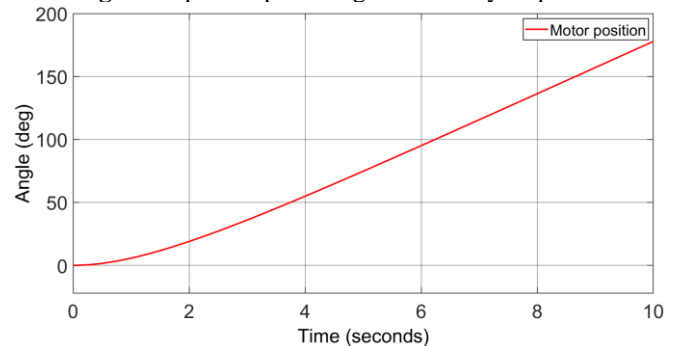


Fig. 11. Open loop test angular position response.

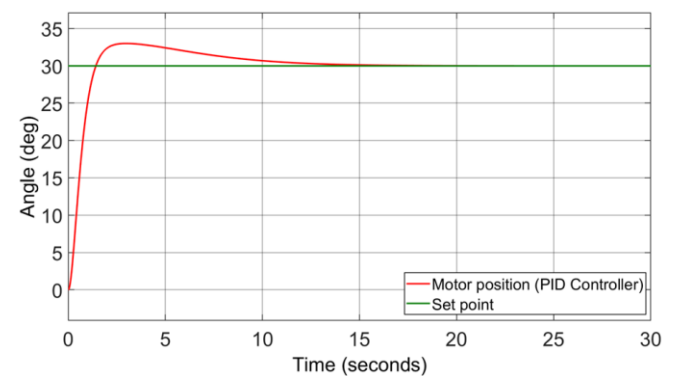


Fig. 12. Motor angle position with PID controller response.

As illustrated in Fig.14, the PID controller is faster at reaching the set point but has a 10% overshoot. In comparison, the Fuzzy PD controller takes slightly longer to get the set point of 8,480 s but provides a more responsive response due to the absence of over-shoot.

3.3. PID and Fuzzy PD Controller Test Result with Measurement Noise Interference

This simulation is run by altering the parameter values in the solar panel system to determine the system's sensitivity to internal uncertainty. Resistance, coil inductance, the moment of inertia, back emf, and torque constant are all changed. The control system is tested for internal disturbances by reducing or increasing the parameter values. The fuzzy PD controller outperforms the PID controller, as illustrated in Fig.15. The fuzzy PD controller is more capable of controlling overshoot and responds faster.

The test results in Fig.15 appear significant when both PID and fuzzy PD controllers are subjected to noise with a variance of 0.1 degrees. In the transient region, the Fuzzy PD controller typically takes longer to reach the set point, which is significantly slower than the condition without measurement noise. In the steady-state area, the two controllers exhibit very similar responses. Table 3 summarizes the characteristics of each system response.

4. Conclusion

In this comparative study, a solar tracking system is used to increase the efficiency of solar energy. PID and Fuzzy PD controllers are used to control the tracking system of the solar panel. The mathematical models of the motor, PID control system, and fuzzy PD control system are presented in Matlab software. The dynamic performance for both controllers is tested separately and alternately, with the rise time for the PID controller being 1.423 s, settling time 22.740 s, and a maximum overshoot of 10%. The fuzzy PD controller has a rise time of 8.480 s, a settling time of 8.480 s, and a maximum overshoot of 0%. Although it has a rise time of 7,057 s, which is longer than the PID controller, the PD fuzzy controller has a settling time of 19,260 s faster than the PID controller. The PD fuzzy controller also has a 0% overshoot, which is very good in the criteria for dynamic response characteristics.

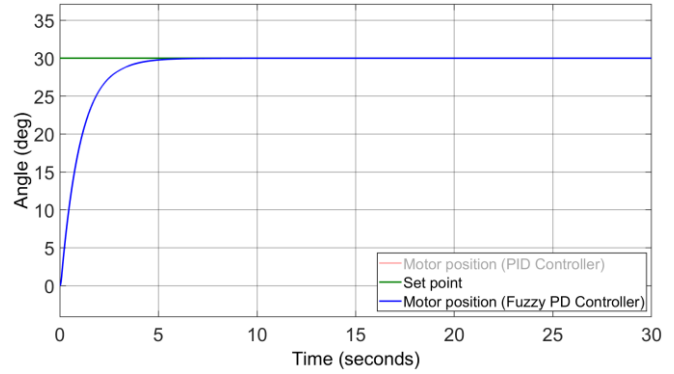


Fig. 13. Motor angle position with Fuzzy PD controller response.

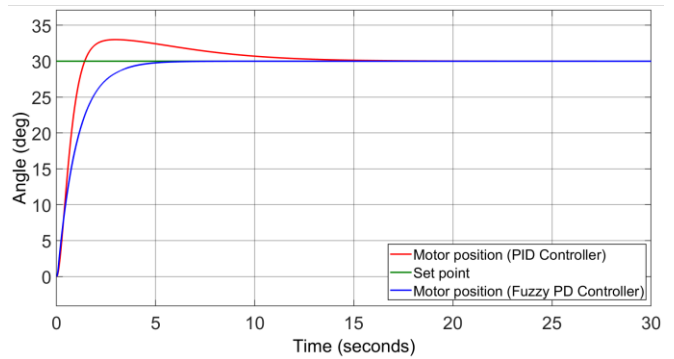


Fig. 14. Comparison of motor angle position response between PID controller and Fuzzy PD.

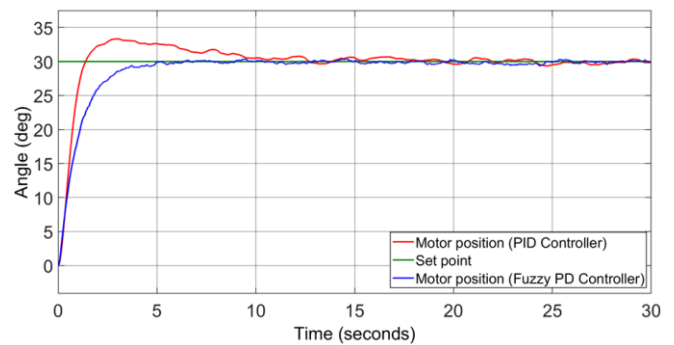


Fig. 15. Comparison of motor angle position response between PID and Fuzzy PD controller with 0.1-degree noise variance.

Table 3. Characteristics of PID and Fuzzy PD control system responses, both without and with interference

Type of Controller	Noise Measurement (degree)	Dead Time (s)	Maximum Overshoot (%)	Settling Time (s)	Rise Time (s)	Steady-State Error
PID	± 0	0.537	10,000	22,740	1.423	0
Fuzzy PD	± 0	0.742	0	8,480	8,480	0.023
PID	± 0.1	0.560	11.100	25,361	1.390	0.116
Fuzzy PD	± 0.1	0.723	0.133	6,388	6,388	0.833

Acknowledgements

This work is supported by The Institution of Research and Community Services National University Jakarta, contract number 3497/LL3/KR/2021, 043/LPPM-UNAS/VII/2021.

References

- [1] L. Miloudi, D. Acheli, and M. Kesraoui, "Application of artificial neural networks for forecasting photovoltaic system parameters," *Applied Solar Energy (English translation of Geliotekhnika)*, doi: 10.3103/S0003701X17020104, vol. 53, no. 2, pp. 85-91, 2017.
- [2] L. M. Elobaid, A. K. Abdelsalam, and E. E. Zakzouk, "Artificial neural network-based photovoltaic maximum power point tracking techniques: A survey," *IET Renewable Power Generation*, doi: 10.1049/iet-rpg.2014.0359, vol. 9, no. 8, pp. 937-942, 2015.
- [3] S. Racharla and K. Rajan, "Solar tracking system—a review," *International Journal of Sustainable Engineering*, doi: 10.1080/19397038.2016.1267816, vol. 10, no. 2, pp. 72-81, 2017.
- [4] R. Singh and R. Banerjee, "Impact of Solar Panel Orientation on Large Scale Rooftop Solar Photovoltaic Scenario for Mumbai," in *Energy Procedia*, doi: 10.1016/j.egypro.2016.11.207, vol. 90, pp. 401-411, 2016.
- [5] S. M. Çınar, F. O. Hocoğlu, and M. Orhun, "A remotely accessible solar tracker system design," *Journal of Renewable and Sustainable Energy*, doi: 10.1063/1.4885099, vol. 6, no. 3, 2014.
- [6] O. Guenounou, A. Belkaid, I. Colak, B. Dahhou, and F. Chabour, "Optimization of fuzzy logic controller based maximum power point tracking using hierarchical genetic algorithms," in *9th International Conference on Smart Grid (icSmartGrid) 2021*, Setubal, pp. 207–211, 29 June-1 July 2021.
- [7] M. Lawan, A. Aboushady, and K. H. Ahmed, "Photovoltaic MPPT Techniques Comparative Review," in *9th International Conference on Renewable Energy Research and Application (ICRERA) 2020*, Glasgow, pp. 344-351, 27-30 September 2020.
- [8] D. S. Ponni A, and Ranjitha R, "Comparison of Efficiencies of Single-Axis Tracking System and Dual-Axis Tracking System with Fixed Mount," *Certified International Journal of Engineering Science and Innovative Technology*, vol. 9001, no. 2, pp. 1925-1933, 2008.
- [9] S. B. Adejuyigbe, B. O. Bolaji, M. U. Olanipekun, and M. R. Adu, "Development of a solar photovoltaic power system to generate electricity for office appliances," *Engineering Journal*, doi: 10.4186/ej.2013.17.1.29, vol. 17, no. 1, pp. 29-39, 2013.
- [10] A. H. Sabry, W. Z. Wan Hasan Mohd Zainal, M. Amran, and S. B. Shafie, "High efficiency integrated solar home automation system based on DC load matching technique," *ARNP Journal of Engineering and Applied Sciences*, vol. 10, no. 15, 2015.
- [11] G. di Francia, "The effect of technological innovations on the cost of the photovoltaic electricity," in *International Conference on Renewable Energy Research and Applications (ICRERA) 2015*, Palermo, pp. 542–546, 22-25 November 2015.
- [12] D. S. Domingues, H. W. Takahashi, C. A. P. Camara, and S. L. Nixdorf, "Automated system developed to control pH and concentration of nutrient solution evaluated in hydroponic lettuce production," *Computers and Electronics in Agriculture*, doi: 10.1016/j.compag.2012.02.006, vol. 84, pp. 53-61, 2012.
- [13] H. S. Grewal, B. Maheshwari, and S. E. Parks, "Water and nutrient use efficiency of a low-cost hydroponic greenhouse for a cucumber crop: An Australian case study," *Agricultural Water Management*, doi: 10.1016/j.agwat.2010.12.010, vol. 98, no. 5, pp. 841-846, 2011.
- [14] G. L. Barbosa et al., "Comparison of land, water, and energy requirements of lettuce grown using hydroponic vs. Conventional agricultural methods," *Int J Environ Res Public Health*, doi: 10.3390/ijerph120606879, vol. 12, no. 6, pp. 6879–6891, 2015.
- [15] J. S. R. Jang and C. T. Sun, "Neuro-Fuzzy Modeling and Control," *Proceedings of the IEEE*, doi: 10.1109/5.364486, vol. 83, no. 3, pp. 378-406, 1995.
- [16] A. Belkaid, I. Colak, K. Kayisli, and R. Bayindir, "Improving PV System Performance using High Efficiency Fuzzy Logic Control," in *8th International Conference on Smart Grid (icSmartGrid) 2020*, Paris, pp. 152–156, 17-19 June 2020.
- [17] Mardlijah and Z. Zuhri, "Solar panel control system using an intelligent control: T2FSMC and firefly algorithm," *Telkomnika (Telecommunication Computing Electronics and Control)*, doi: 10.12928/TELKOMNIKA.v16i6.8694, vol. 16, no. 6, pp. 2988-2998, 2018.
- [18] M. A. Tankari, D. Gueye, and A. H. Ndiaye, "Design Methodology of Novel PID for Efficient Integration of PV Power to Electrical Distributed Network," *International Journal of Smart grid*, doi: 10.20508/ijsmartgrid.v2i1.14.g11, vol. 2, no. 1, pp.77-86, 2018.
- [19] F. Hidayanti, "Design of Single-Axis Solar Tracker based on Arduino Uno Microcontroller," *International Journal of Emerging Trends in Engineering Research*, doi: 10.30534/ijeter/2020/07842020, vol. 8, no. 4, 2020.
- [20] F. Hidayanti, "Dual-Axis Solar Tracking System Efficiency for Hydroponics Pump," *International Journal of Emerging Trends in Engineering Research*, doi: 10.30534/ijeter/2020/67862020, vol. 8, no. 6, 2020.

- [21] J. M. Wang and C. L. Lu, "Design and implementation of a sun tracker with a dual-axis single motor for an optical sensor-based photovoltaic system," *Sensors* (Switzerland), doi: 10.3390/s130303157, vol. 13, no. 3, 2013.
- [22] S. Padhee, U. C. Pati, and K. Mahapatra, "Design of photovoltaic MPPT based charger for lead-acid batteries," in *IEEE International Conference on Emerging Technologies and Innovative Business Practices for the Transformation of Societies (EmergiTech) 2016*, Balaclava, pp. 351-356, 3-6 August 2016.